Atlas Based Segmentation of the prostate in MR images

Albert Gubern-Merida and Robert Marti

Universitat de Girona, Computer Vision and Robotics Group,
Girona, Spain
{agubern,marly}@eia.udg.edu

Abstract. The large variability and contrast differences between prostates make its segmentation difficult using traditional segmentation methods. In this paper we present an automatic method based on nonrigid registration of a set of prelabelled MR altas images. The algorithm consists of three stages. Firstly, the target image is nonrigidly registered with each atlas image, using mutual information as the similarity measure. Subsequently, the best registered image is selected comparing normalised mutual information measures after registration. Finally, the segmentation is obtained by deforming the corresponding atlas labelled image selected before using the transformation determined on the registration stage. The method is evaluated on 15 images using the Dice similarity coeficient and 95% Hausdorff distance, obtaining medians of 0.79 and 7.11 mm respectively.

Key words: image segmentation, image registration, atlas matching, magnetic resonance imaging, prostate

1 Introduction

In this work we have implemented an automatic segmentation method based on atlas matching that, in contrast to traditional segmentation techniques, allows to take the large variability and the contrast differences of the prostates into account. The atlas consists of a set of images with their respective labelled image manually provided by an expert. The segmentation method is based on the work of Klein et al. [1] but also introduces some modifications which are described in the Sec 2. The method is evaluated using 15 MRI T2 images (Sec. 3), following the guidelines of the prostate segmentation challenge held within the MICCAI 2009 conference. The aim of this work is to evaluate the atlas based segmentation methods using a common evaluation framework in order to be comparable to the other published approaches. The paper finally presents the discussion, conclusions and future directions.

2 Method

The method consists of three stages: first a registration of all atlas images to the patient image that will be segmented, selection of atlas image that matches

best with the patient image, and finally the deformation of the corresponding atlas label image using the transformation obtained in the registration stage. Referring to the last two stages, due to the small number of images to test and the large variability among them, we have selected only one matching image so no combination of segmentations is used in contrast with the work presented by Klein et al. [1].

In the presented method, a set of N accurately labelled images, which serve as an atlas, are assumed to be available. The ith image in this atlas set is referred to as $A_i(x)$. The corresponding label image is called $L_i(x)$, a binary image where 'ones' represent prostate tissue and 'zeros' everything else. The new image to be segmented is denoted by $P(x)$. The goal of the automatic segmentation method is to produce a label image $\hat{L}_P(x)$ that accurately defines the prostate of the patient. Ideally, this label image should be equal to a manual segmentation $L_P(x)$ created by an expert.

2.1 Registration

In the registration stage, each atlas image A_i is matched to the image P to be segmented. A coordinate transformation $T_i(x)$ is estimated that maximises the similarity of P and the deformed atlas $A_i \circ T_i$. We use here *mattes mutual information* as a measure of similarity [2]. Figure 1 shows a schematic representation of this stage.

Before registration, a rectangular region of interest the prostate where appears is extracted in the images in order to focus the registration process. In altas images, this region is delimited by a bounding box automatically obtained from its respective labelled image. The patient the region is selected manually that is the only step in the method that requires user intervention. Doing this extraction we have observed that even the effects of severe intensity inhomogeneity caused by magnetic field artifacts are minised, therefore bias field correction was not deemed to be needed.

The registration process itself is performed in three steps. Firstly, global pose differences are compensated for by an affine registration algorithm. Subsequently, a nonrigid registration is performed, using a coordinate transformation that is parameterised by cubic B-Splines [3]. In this second step a small number of control grid points is defined to model global nonrigid deformations. Finally, a second nonrigid registration is performed in order to model highly local nonrigid deformations defining large number of control grid points. For the main test 5 and 10 control grid point values are the selected.

The transformation that maximises the similarity measure is estimated by an iterative stochastic gradient descent optimisation.

2.2 Atlas selection

In this stage, we need to select the registered atlas image which is more similar to the patient's image as shown in figure 2.

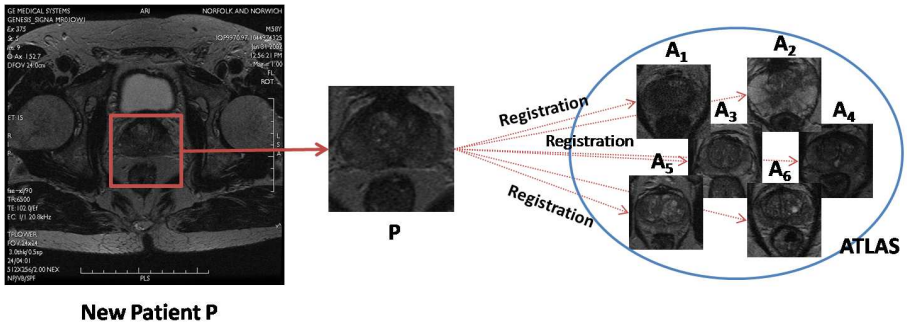

Fig. 1. First stage: each atlas image is matched to the patient image

The similarity measure used is a normalization of mattes mutual information (see equation 1) taking into account for each pair of registered images (A and B) the entropy of the fixed image $H(A)$. The use of this metric has in consideration the differences of number of pixels between the registered images. The measure is computed on the extracted regions before registration stage.

$$NMI(A,B) = \frac{MI(A,B)}{H(A)} \tag{1}$$

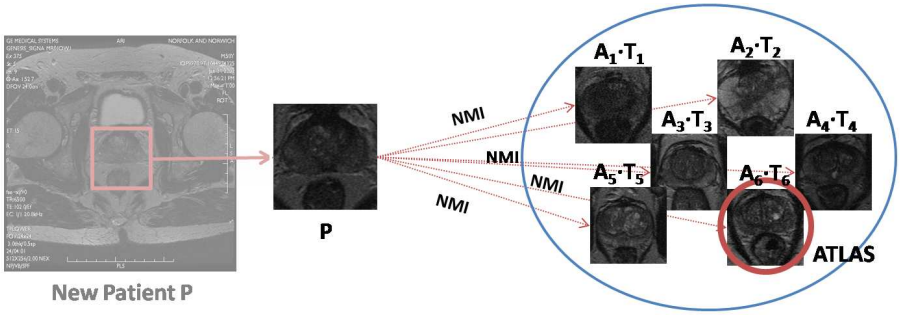

Fig. 2. Second stage: selection of the image that best matches the patient image

2.3 Label image deformation

In the third stage, the label image corresponding to the chosen atlas image A_i is deformed. Coordinate transformation T_i obtained in the registration stage is applied $L_i \circ T_i$ in order to get the segmentation of the patient's image $\hat{L}_P(x)$. Figure 3 illustrates this stage.

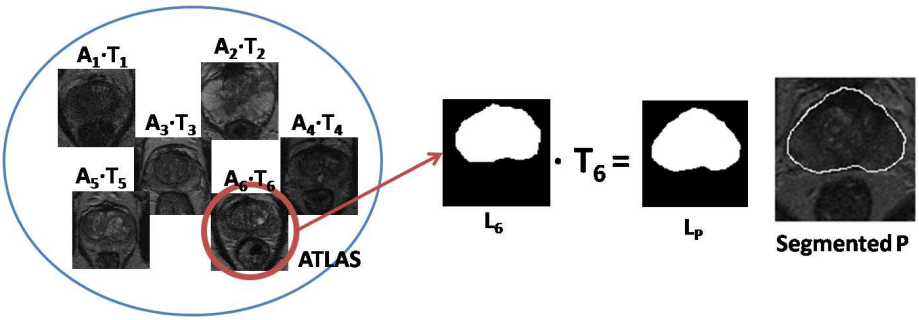

Fig. 3. Third stage: deformation of the labelled image

3 Results

The proposed automatic segmentation method has been implemented using ITK libraries [4] and are evaluated using the set of 15 T2 images of the trainning data. Each image has been segmented building an atlas with the rest of the 14 MR images (following a leave-one-out scheme). Quantitative evaluation is done comparing the automatically generated segmentations with the manual segmentations provided by an expert. The measures to evaluate the segmentations are the Dice similarity coefficient (DSC) [5] and 95% Hausdorff distance (HD) [6]. Moreover, slices of MR images with their segmentation are shown providing a qualitative evaluation. The method has tested on a workstation with four Quad-Core AMD Opteron(tm) Processor 8378 and 128 GB RAM. The execution time to run each segmentation is about 60 minutes approximately.

Figure 4.(a) compares the DSC and 4.(b) the HD values for each test volume. On one hand, having in mind it is generally accepted that a value of DSC > 0.7 represents excellent agreement [7], the median DSC value of 0.79 confirms the overall satisfactory results of the segmentations. On the other hand, the median HD value is 7.11 mm. We consider this value as acceptable, especially taking into account that the axial spacing in images are 5 mm and the average prostate volume is about 40 cm^3.

Confirming and exemplifying the quantitative analysis above, figure 5 shows some slices of each segmentation with DSC values greater than 0.7 (13 out of 15). In most of images it is possible to observe that the contour correctly delimits the prostate in accordance with their respective DSC and HD values.

Referring to unsatisfactory results with DSC < 0.7 (images 45 and 88), we have seen that the result in image 45 could be explained by the difficulty of finding a similar prostate in the atlas. This illustrates the fact that registration stage works correctly handling deformations up to a certain magnitude. On the other hand, the problem in image 88 seems to be explained by an incorrect registration result. In this case we have obtained a better segmentation (DSC $=$ 0.76 and HD $= 6.01$ mm) using 15 control points in the last nonrigid registration step instead of 10. However, using these parameters for all the segmentations,

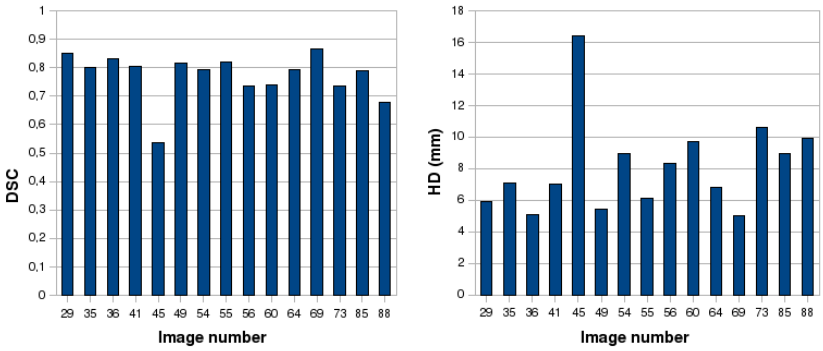

(*a*) **DSC** (*b*) **HD**

Fig. 4. (*a*) DSC and (*b*) HD values for each test volume

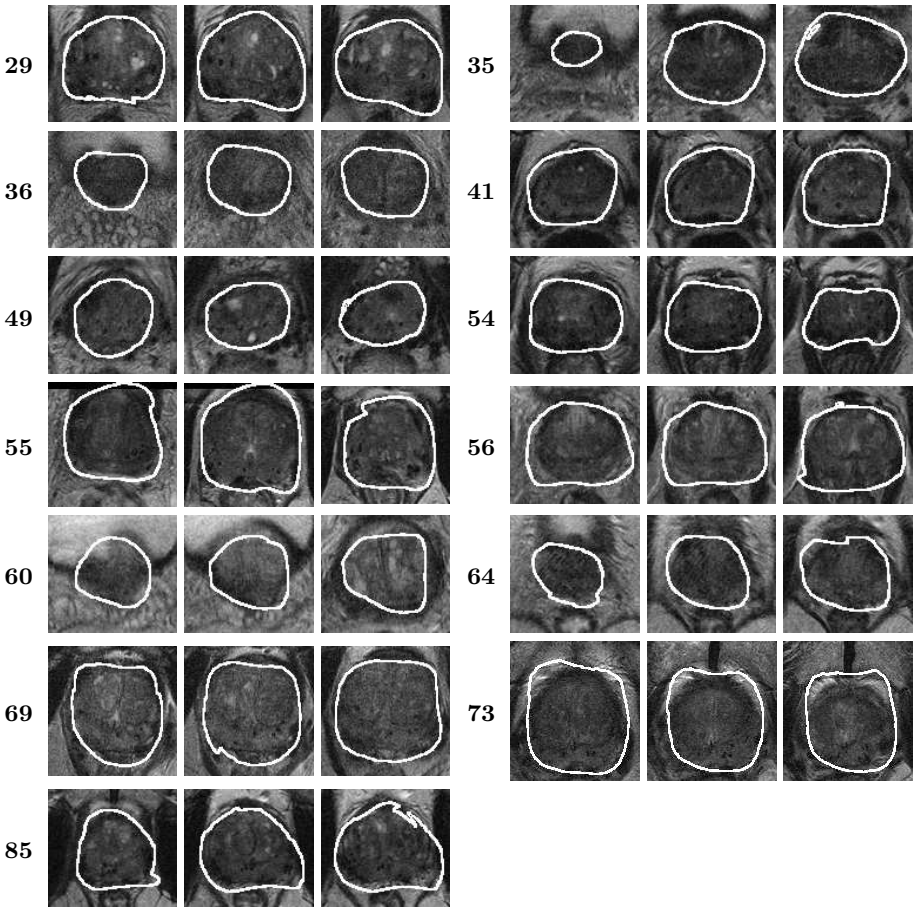

Fig. 5. Example slices of each prostate segmentation with DSC > 0.7

the median DSC and HD values are slightly lower (DSC = 0.76 and HD = 8.48 mm). It should be noted that even with those registration parameters, the segmentation of image 45 was still unsatisfactory confirming the need of a larger atlas database as mentioned before.

4 Conclusions

In this work an automatic prostate segmentation method of MR images has been investigated. The method is based on matching a set of manually segmented images taking into account the large variability and contrast differences of the prostates.

Evaluation has been performed using the 15 T2 MR images of the training data. A leave one out methodology has been used for each segmentation: one image is segmented building an atlas with the rest of the 14 volumes. The obtained segmentations are compared to a manual segmentation using the Dice similarity coefficient and 95% Hausdorff distance (HD) achieving acceptable results with medians of 0.79 and 7.11 mm respectively. The visual results shown also confirm the DSC and HD values observing a good delineation of the prostate region.

We have noted some important points concerning the behaviour of the prostate segmentation method based on atlas matching. Firstly, atlas needs to contain a representative variation of images. If the patient image to be segmented has a similar one into atlas, the segmentation result will be better because the registration stage will be able to handle the differences between prostates more effective and easily. For this reason, adding more images into the atlas and the optimization of the atlas composition are regarded as important future works. Moreover, we have observed different segmentation results depending on the number of control points in the nonrigid registration step, not achieving the best results with the same value. Therefore, future work also includes an optimitzation of registration stage to better adjust the registration parameters in order to obtain the best results.

Acknowledgments. This work was supported by the Ministerio de Educacion y Ciencia of Spain under Grant TIN2007-60553, by the UdG under Grant IdIBGi-UdG, by the CIRIT and CUR of DIUiE of Generalitat de Catalunya under grant 2008SALUT00029 and by the CIDEM under VALTEC08-1-0039 .

References

1. Klein, S., van der Heide, U., Raaymakers, B., Kotte, A., Staring, M., Pluim, J.: Segmentation of the prostate in MR images by atlas matching. In: International Symposium on Biomedical Imaging. (April 2007) 1300–1303
2. Mattes, D., Haynor, D., Vesselle, H., Lewellen, T., Eubank, W.: Pet-ct image registration in the chest using free-form deformations. **22**(1) (January 2003) 120–128

3. Rueckert, D., Hayes, C., Studholme, C., Summers, P., Leach, M., Hawkes, D.J.: Non-rigid registration of breast mr images using mutual information. Proc. Medical Image Computing and Computer-Assisted Intervention MICCAI'98 (1998) 1144–1152
4. Ibanez, L., Shcroeder, W., Ng, L., J.Cates, the Insight Software Consortium: ITK - Segmentation & Registration Toolkit. `www.itk.org` (May 2009)
5. Bharatha, A., Hirose, M., Hata, N., Warfield, S.K., Ferrant, M., Zou, K.H., Suarez-santana, E., Ruiz-Alzola, J., D'Amico, A., Cormack, R.A., Kikinis, R., Jolesz, F.A., Tempany, C.M.C.: Evaluation of three-dimensional finite element-based deformable registration of pre- and intra-operative prostate imaging (2001)
6. Archip, N., Clatz, O., Whalen, S., Kacher, D., Fedorov, A., Kot, A., Chrisochoides, N., Jolesz, F., Golby, A., Black, P., Warfield, S.: Non-rigid alignment of preoperative MRI, fMRI, and DT-MRI with intra-operative MRI for enhanced visualization and navigation in image-guided neurosurgery. Neuroimage **35**(2) (April 2007) 609–24
7. Zijdenbos, A.P., Dawant, B.M., Margolin, R.A., Palmer, A.C.: Morphometric analysis of white matter lesions in mr images: method and validation. Medical Imaging, IEEE Transactions on **13**(4) (1994) 716–724